

VUV and low energy electron impact study of electronic state spectroscopy of CF₃I

N.J. Mason^{a,*}, P. Limão Vieira^{a,1}, S. Eden^a, P. Kendall^a, S. Pathak^{a,2}, A. Dawes^a, J. Tennyson^a, P. Tegeder^a, M. Kitajima^b, M. Okamoto^b, K. Sunohara^b, H. Tanaka^b, H. Cho^c, S. Samukawa^d, S.V. Hoffmann^e, D. Newnham^f, S.M. Spyrou^g

^a Department of Physics and Astronomy, University College London, Gower Street, London WC1E 6BT, UK

^b Department of Physics, Sophia University, Chyoicho 7-1, Chiyoda-ku, Tokyo 102-8854, Japan

^c Department of Physics, Chungnam National University, Taejeon, South Korea

^d Institute of Fluid Science, Tohoku University, 2-1-1 Katahira Aoba-ku, Sendai 980-8577, Japan

^e Institute for Storage Ring Facilities, University of Aarhus, Ny Munkgade, DK-8000 Aarhus C, Denmark

^f Molecular Structure Facility, Rutherford Appleton Laboratory, UK

^g Theoretical & Physical Chemistry Institute, National Hellenic Research Foundation, 48 Vas. Constantinou Ave., Athens 116 35, Greece

Received 14 February 2002; accepted 15 June 2002

Abstract

The electronic states of CF₃I have been investigated using photon and electron energy loss spectroscopy from 4 to 20 eV (310 nm > λ > 60 nm). Assignments have been suggested for each of the observed absorption bands incorporating both valence and Rydberg transitions. Vibrational structure in each of these bands is observed for the first time. Absolute photo-absorption cross-sections have also been measured and are compared with earlier measurements. (Int J Mass Spectrom 223–224 (2003) 647–660)

© 2002 Elsevier Science B.V. All rights reserved.

Keywords: VUV absorption; Electron energy loss; Spectroscopy; Synchrotron radiation; Aeronomy

1. Introduction

In the manufacture of ultra-large-scale-integrated circuits, it is necessary to fabricate predetermined patterns on a scale of less than 0.1 μm and fine structures with an aspect ratio of more than 10 on

a silicon wafers with diameters of greater 30 cm. This process requires a well-collimated, spatially uniform, high-density plasma source operating under low-pressure conditions [1]. The main feed gases used by the plasma etching industry are perfluorocarbons (CF₄, C₂F₆, C₃F₈, CHF₃, and c-C₄F₈) however, these are also strong greenhouse gases and therefore, under the terms of the Kyoto Protocol, must be replaced by alternative compounds that have low 'global warming potentials' [2]. One possible replacement is CF₃I since, due the weak C–I bond, it should be possible

* Corresponding author. E-mail: nigel.mason@ucl.ac.uk

¹ On leave from Departamento de Física, FCT-UNL, P-2829-516 Caparica, Portugal and Centro de Física Molecular, Complexo I, IST, Av. Rovisco Pais, P-1049-001 Lisboa, Portugal.

² Permanent address: Christchurch College, Kanpur, India.

to produce high yields of CF_3 radical in any etching plasma by direct electron impact dissociation of CF_3I . However, at present, there is a lack of data on both the electronic state spectroscopy of CF_3I and absolute photo-absorption cross-sections, a situation that prevents a full simulation of the applicability of CF_3I to plasma research.

Sutcliffe and Walsh [3] were the first to report a vacuum-ultraviolet (VUV) absorption spectrum of CF_3I in the wavelength range from 110 to 180 nm. Shortly afterwards Herzberg [4] extended this work and made the first tentative assignment of observed absorption bands. Subsequently, Fuss [5] combined ultraviolet radiation to excite CF_3I in the range 174–180 nm with a pulsed CO_2 laser to excite the molecule in its vibrational absorption bands. Powis et al. [6] reported dissociative photoionisation of CF_3I as well as threshold photoelectron spectroscopy for photon energies from 10 to 32 eV. Taatjes et al. [7] and Macleod et al. [8] reported resonant-enhanced multiphoton ionisation (REMPI) spectra of CF_3I and measured photoelectron spectra.

Despite these measurements a full high resolution photo-absorption spectrum of CF_3I has yet to be recorded and the absorption bands assigned to valence and Rydberg transitions. Nor are quantitative absolute photo-absorption cross-sections available to determine the photolysis rate (and thence global warming potential) of CF_3I in the terrestrial atmosphere, indeed two long wavelength photo-absorption cross-section measurements of the lowest absorption band are in considerable disagreement [9–11]. Thus, we have performed an exhaustive series of measurements to determine both the absolute photo-absorption cross-section of CF_3I and to probe its electronic spectroscopy over the energy range from 4 to 13.5 eV ($310 \text{ nm} > \lambda > 90 \text{ nm}$).

2. Experimental apparatus

Two experimental methods were used out to investigate the electronic spectroscopy of CF_3I . The photo-absorption technique, to measure absolute ab-

sorption cross-sections and the electron energy-loss spectrum (EELS) technique to measure the EELS which under well defined collisions conditions may be compared directly with the photo-absorption cross-section.

2.1. Photo-absorption spectra

The photo-absorption spectra were recorded using synchrotron radiation on the ultraviolet vacuum line (UV1) of the ASTRID facility³ at Aarhus University, Denmark. The apparatus used consisted of a simple static gas cell with an absorption path length of 15 cm and with a photomultiplier to record the transmitted light, I_t at 0.05 nm intervals. The typical resolution was 0.075 nm. As well as the transmitted light intensity, the sample pressure (measured on an MKS 390HA Baratron capacitance manometer, $\pm 0.1\%$) and the synchrotron beam ring current were monitored at each wavelength. The sample cell was then evacuated and the radiation transmitted through the empty cell, I_0 , measured absolute photo-absorption cross-section may then be derived using the Beer–Lambert law:

$$I_t = I_0 \exp(-n\sigma x) \quad (1)$$

where n is the target gas number density, σ the absorption cross-section, and x is the path length [12]. The minimum wavelength for which data could be collected is determined by the choice of entrance and exit windows in the gas cell. The present configuration uses a LiF entrance window and a CaF_2 exit window in front of the photomultiplier tube, hence the lowest wavelength at which reliable data could be collected is 115 nm. To ensure that the data was free of any saturation effects [13], the cross-section was measured over the pressure range 0.04–0.75 Torr with typical attenuation of less than 10%. Precautions were also taken in both experiments to avoid any second-order light effects.

In addition, in order to measure absolute cross-sections at low incident energies (long wavelengths) we also used the Molecular Structure Facility (MSF)

³ <http://www.isa.au.dk/SR/UV1/uv1.html>.

at the UK Rutherford Appleton Laboratory (RAL). Ultraviolet photo-absorption cross-sections of CF_3I were measured by means of a high resolution Fourier transform spectrometer. The Bruker IFS 120HR FTS has a maximum optical path of 6 m and was operated at a spectral resolution of 0.25 cm^{-1} . The beam exits the spectrometer through a wedged calcium fluoride window and enters two connected stainless-steel vacuum chambers (kept at a pressure below 10^{-3} hPa), containing the sample, a pyrex glass cell (path length 22.824 cm), UV detector and other optical components. Gas samples were introduced into the absorption cell and were isolated for the duration of the spectroscopic measurements. These were carried out over several different spectral regions between 225 and 400 nm with six scans per run. For each range, background spectra were obtained with the cell evacuated, before and after sample spectrum. The temperature dependence of the cross-section was studied using the MSF instrument at 296, 272, and 259 K for the wavelength range 250–310 nm.

2.2. Electron energy-loss spectra

Electron energy-loss spectroscopy provides an alternative methodology for probing the excited states of atoms and molecules. At large scattering angles and low incident energies forbidden transitions dominate the observed EELS while at small scattering angles and high incident energies allowed transitions are dominant [14]. If an EELS is recorded at electron energies in excess of 100 eV and at scattering angles close to zero degrees the EELS spectrum may be directly compared with a photo-absorption cross-section. We have used this technique to derive photo-absorption cross-sections for many molecules in the FUV, beyond the optical cut off of the LiF window in our gas cell [15] and in this paper, we use the technique to explore the photo-absorption cross-section of CF_3I above 11 eV.

EELS spectra have been recorded using two standard high resolution instruments (typically 35–50 meV). One at University College London [16], the other at Sophia University, Tokyo, Japan [17]. Briefly,

electrons from a 180° monochromator intercept an effusive molecular beam at right angles, and scattered electrons are energy analysed in a second 180° hemispherical system. A set of electron lenses in the electron spectrometer is used for imaging and energy control of the electron beam, whose characteristics were confirmed by electron trajectory calculations. The target molecular beam is produced by effusing CF_3I through a simple nozzle. The analyser can be rotated around the scattering centre covering an angular range from -10 to 130° with respect to the incident electron beam. The overall energy-resolution of the present measurements is 35–40 meV, and the angular resolution is $\pm 1.5^\circ$.

The CF_3I gas was purchased from Argo international for the European experiments and from Takachiho Chemicals Co. Ltd. for the experiments performed in Japan all gases were quoted to have a purity of greater than 99.999% and was used without further purification or treatment.

3. Results and discussion

3.1. Spectroscopy of CF_3I

The photo-absorption spectrum may be characterised by three regions (Fig. 1): one very weak continuum around centred about 4.7 eV; a second region consisting of five prominent band structures observed at around 7.4, 8.1, 9.0, 9.8, and 10.3 eV all of which are found to contain rich vibrational structure (Fig. 1(a)–(e)). The third region above the ionisation potential shows some broader featureless peaks. The sharp fall in cross-section above 10.5 eV is an experimental artefact due to the cut off transmission of the CaF_2 window.

Electron energy-loss spectra (4–13.5 eV) are shown in Fig. 2. The lowest band is more enhanced at lower incident electron energies—a trend characteristic of forbidden transitions, while the next five bands show greater differential cross-sections at higher incident electron energies—a trend characteristic of optically allowed transitions.

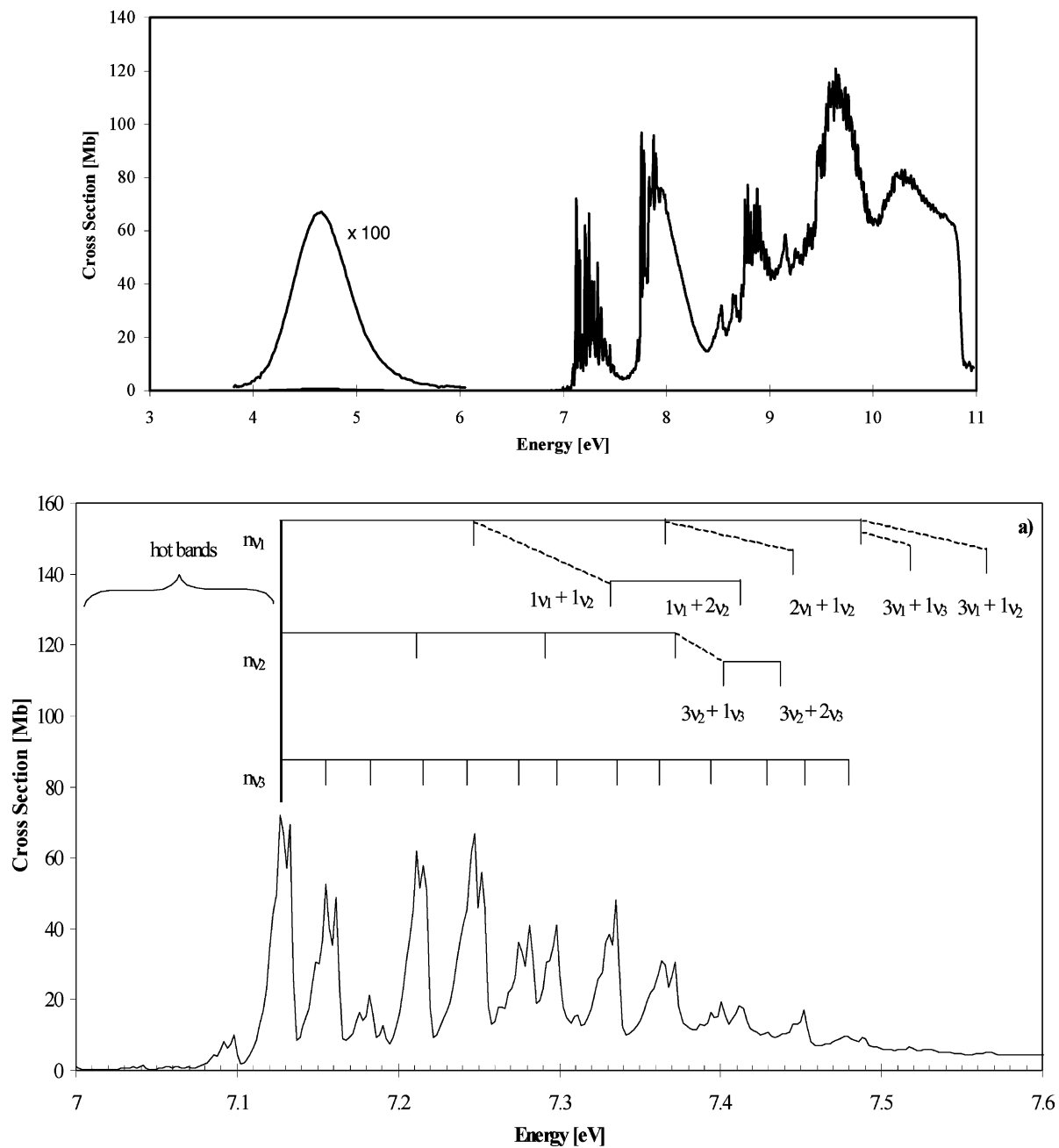


Fig. 1. High-resolution total photo-absorption spectrum of CF_3I from recorded on the ASTRID Synchrotron ring facility. Photo-absorption spectrum in the 7.0–7.6 eV (a), 7.6–8.3 eV (b), 8.5–9.1 eV (c), 9.1–10.0 eV (d), and 10.0–11.0 eV (e), respectively, absorption band of the CF_3I .

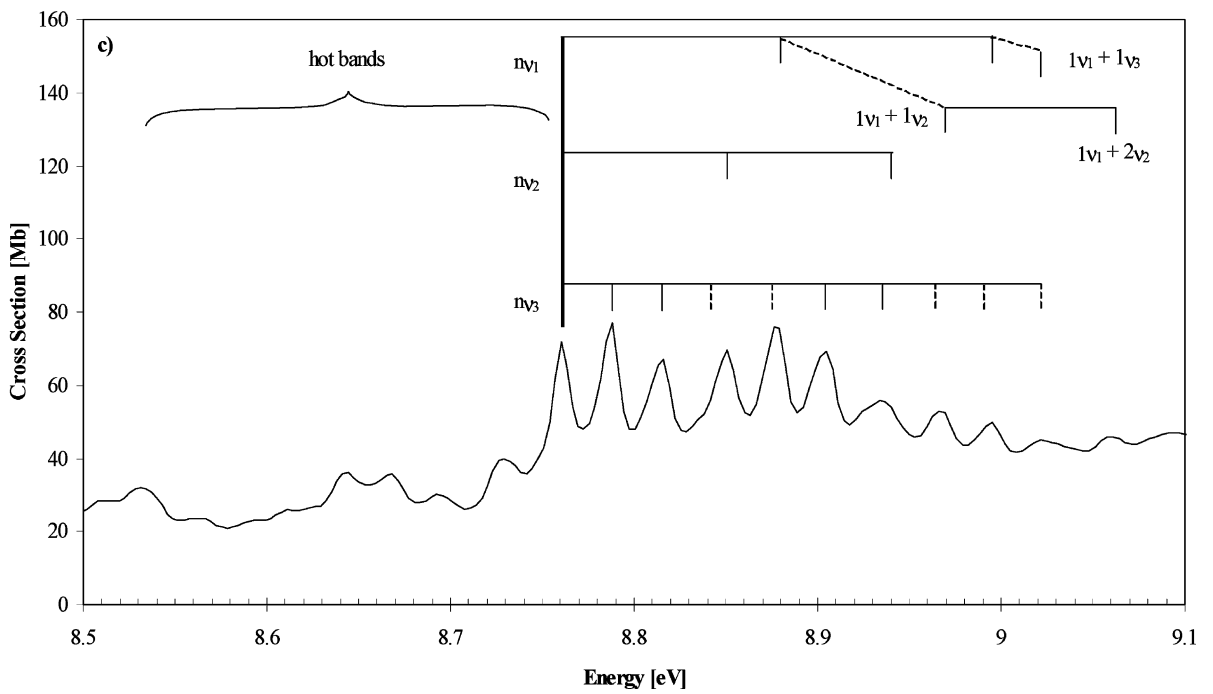
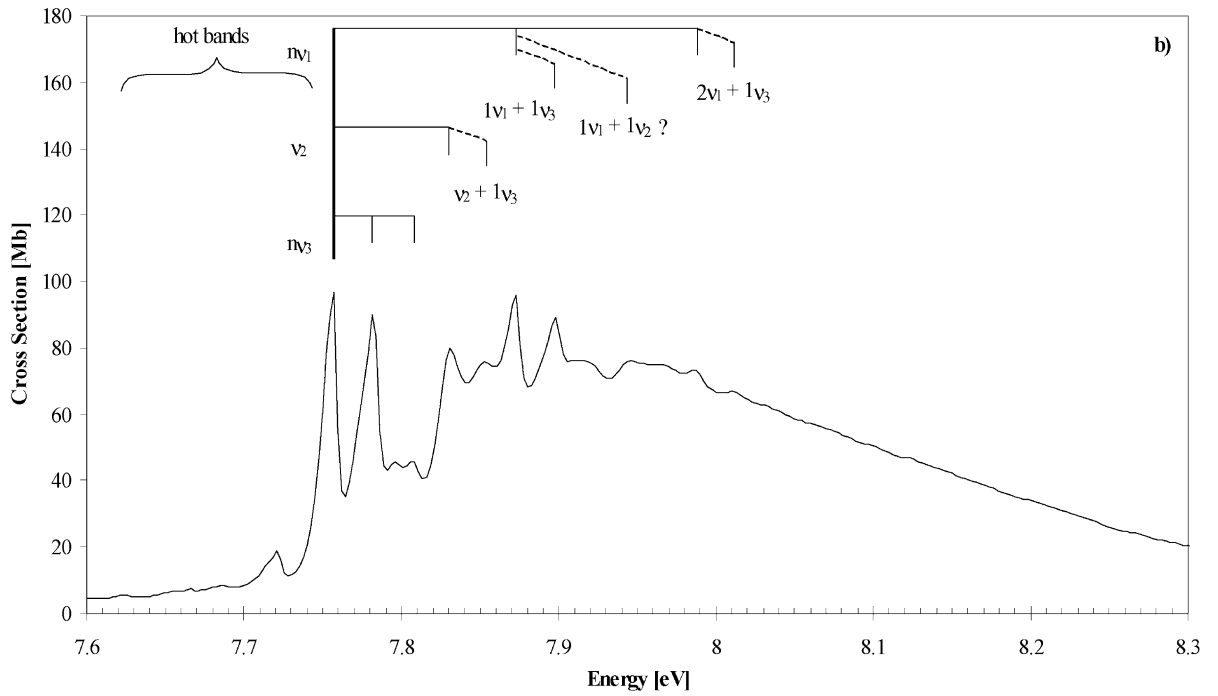


Fig. 1. (Continued).

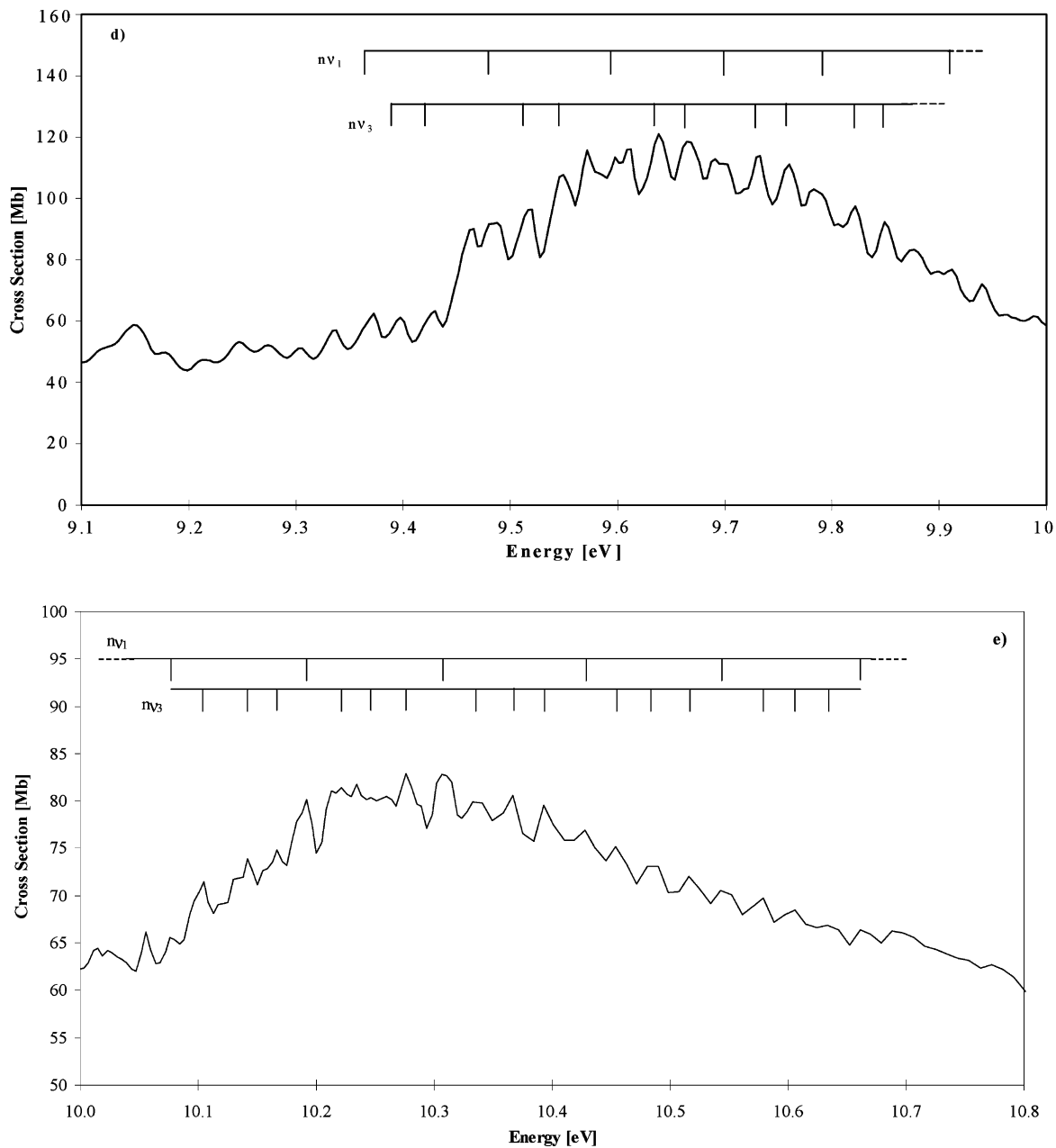


Fig. 1. (Continued).

A brief review of the structure, geometry and properties of CF₃I is helpful in the analysis and interpretation of the present and other literature data. CF₃I is a symmetrical top of symmetry C_{3v}. The six vibrational normal modes are classified in the symmetry types

$\Gamma_{\text{vib}} = 3A_1 + 3E$, where, according to Herzberg's [18] notation, $\nu_1 = 0.133$, $\nu_2 = 0.092$, $\nu_3 = 0.036$, $\nu_4 = 0.147$, $\nu_5 = 0.067$, and $\nu_6 = 0.033$ eV. Its ground electronic state is totally symmetric A₁. According to Taatjes et al. [7] the highest occupied orbital (HOMO)

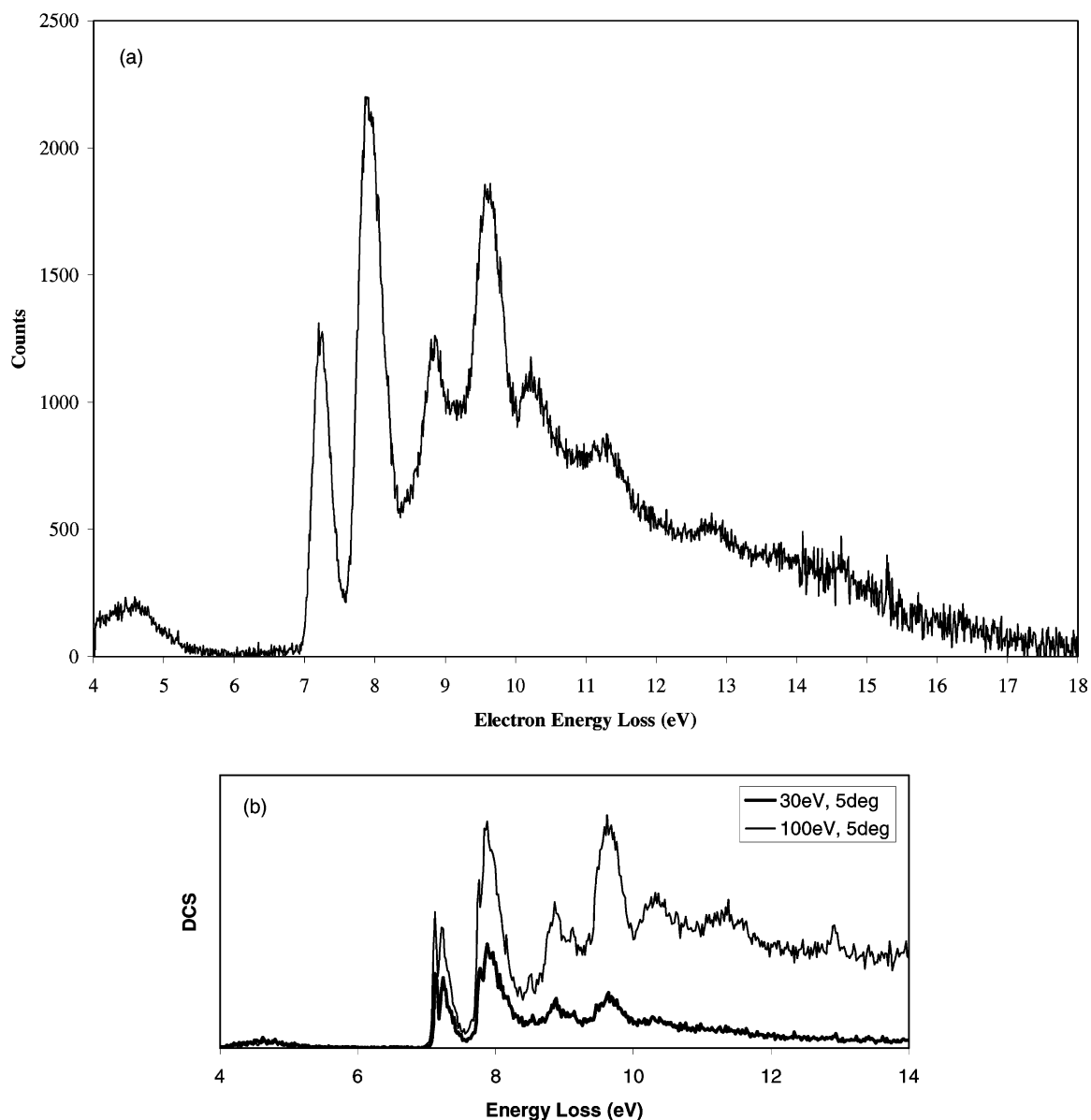


Fig. 2. Electron energy loss spectra of CF_3I measured: (a) at University College London with an incident electron energy of 150 eV and at scattering angle 0° (b) at Sophia University, Tokyo CF_3I at a scattering angle of 5° and incident energies of 30 and 100 eV.

in CF_3I was found to be the iodine lone pair (n) orbital (which has a spin-orbit splitting of 5030 cm^{-1}), followed by the C–I bonding orbital (σ). The C–F bonding orbitals and the fluorine lone pairs are much more strongly bound. The lowest unoccupied orbital (LUMO) has mainly C–I anti-bonding character (σ^*),

while the next unoccupied orbital is a diffuse one of mostly iodine 6s character.

The lowest energy excitations are shown in Table 1. In these transitions, an electron is removed from 5p degenerate, lone-pair orbitals of the iodine atom and placed in the 6s orbital of the iodine atom. This

Table 1
Experimental transition energies of CF₃I (energies in eV)

Transition type	Excited state	This work	[7]
n → σ*	² E _{3/2} [2]	4.627	4.675
	² E _{3/2} [1]		
	² E _{1/2} [0]		
	² E _{1/2} [1]		
σ → σ*	³ A ₁ [0 + 1]	–	6.154 ^a
	¹ E ₁ [1]	7.831	7.837
n → 6s	² E _{3/2} [2]	–	7.052
	² E _{3/2} [1]	7.126	7.130
	² E _{1/2} [0]	–	7.650
	² E _{1/2} [1]	7.757	7.754

^a Theoretical calculation.

transition is split due to the spin–orbit coupling of the iodine atom, a similar feature has been observed in the related molecule—methyl iodide, CH₃I [19]. The ion core states ²E_{3/2} and ²E_{1/2} are thus, split into states with projections of the total electronic angular momentum Ω of 2, 1, 0, 1. Upon coupling with the Rydberg electron, the ²E_{3/2} (ionic \tilde{C} state) produces ²E_{3/2} [2] and ²E_{3/2} [1], and the ²E_{1/2} (ionic \tilde{D} state) produces ²E_{1/2} [0] and ²E_{1/2} [1] states.

The absorption features observed above 6.8 eV (Fig. 1(a)–(e)), can be interpreted as Rydberg series converging to the CF₃I⁺ ground state doublet, $\tilde{X}^2E_{3/2}$ and $\tilde{X}^2E_{1/2}$ arising from the transition of a

lone-pair iodine electron to the Rydberg orbital 6sa₁. Between 7 and 8 eV, the two most intense peaks, at 7.126 and 7.757 eV have been assigned to the 0–0 transitions from the ¹Σ⁺ ground state to the ²Π_{3/2} and ²Π_{1/2}. Similar features are also observed in the photo-absorption cross-section of CH₃I albeit at shorter wavelengths [20]. The 0.631 eV energy separation is of the same order as the spin–orbit coupling in the ground state of the iodine atom. These transitions will be discussed in detail later.

3.2. The A band (3.5–6.5 eV region)

The broad and weak continuous $\tilde{A} \leftarrow \tilde{X}$ absorption feature centred around 4.6 eV (266 nm) with a local maximum cross-section of 0.67 Mb is a result of the excitation to an anti-bonding orbital along the C–I bond (n → σ*) of the CF₃I molecule.

As mentioned above, special attention has been devoted to the photodissociation studies on CF₃I because excitation in the A band (350–200 nm) results in prompt dissociation along the C–I bond due to the strong *repulsive nature* of the excited state, i.e., dissociation into a ground-state (fluorinated)-alkyl radical (CF₃) and a ground-state I (=I (²P_{3/2})) and excited-state I* (=I (²P_{1/2})) and hence provides a

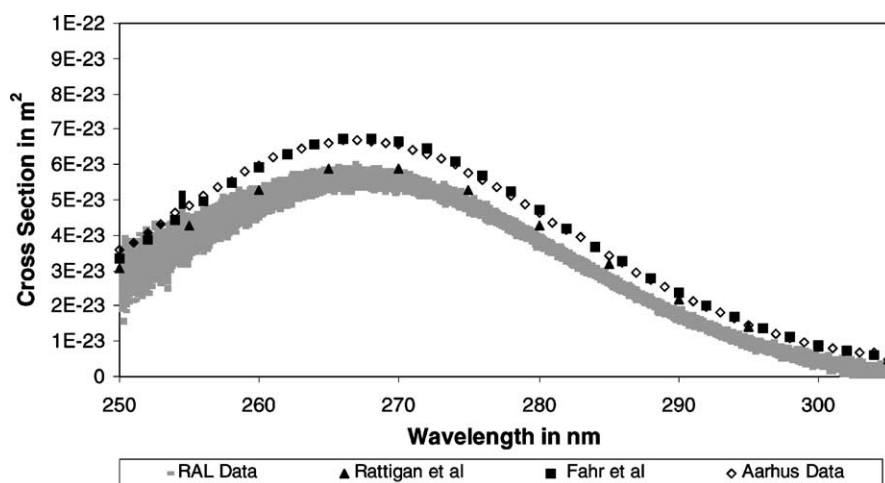


Fig. 3. Photo-absorption cross-section of the lowest band in CF₃I showing data Recorded at ASTRID (◇); At the MSF, Rutherford Laboratory (---) compared with previous data of Rattigan and Cox (▲) and Fahr et al. [9] (■).

source of radicals for etching silicon wafers in industrial plasma reactors. This band has been also observed by Fuss [5] at 267 nm and was probed by van den Hoek et al. [21] using REMPI spectroscopy and Waits et al. [22] who observed I^+ formation via the parent ion photodissociation, while CF_3^+ ion is formed via thermal decomposition of the parent as well as parent ion photodissociation.

Absolute photo-absorption cross-sections for the A band have been reported in three earlier experiments [9–11] but disagree in the magnitude of the cross-section. The photo-absorption cross-sections recorded at the MSF are some 10% lower than the results of Solomon et al. [11] and Fahr et al. [9] but agree with those of Rattigan et al. [10] (Fig. 3). In contrast, the cross-sections derived from the ASTRID synchrotron agree well with the data of Solomon et al. and Fahr et al. but not those of Rattigan et al. Preliminary measurements taken at the UK Daresbury facility produced photo-absorption cross-sections that are in good agreement ($\pm 10\%$) with those taken on ASTRID.

No evidence for temperature dependence between 259 and 296 K was observed in the wavelength range studied (250–310 nm). This is consistent with Fahr et al. [9] reporting a maximum fall of 10% in A band cross-section as temperature is increased from 253 to 293 K. This difference is less than the experimental uncertainty indicated by the thickness of the presented curve in Fig. 3.

3.3. The B band

In the B band, the main peak is centred at 7.126 eV and assigned as a 0–0 transition for the origin of $^2E_{3/2}$ [1] state [7]. This band exhibits fine structure dominated by three vibrational progressions. Energy values are tabulated and compared with other literature data [3,7] in Table 2. The vibrational structure has been attributed mainly to the progression of the C–I stretching mode (ν_3) [3]. However, we observe other vibrational progressions in this region involving both ν_2 and ν_3 and it seems that an excitation of the F_3 –C–I bending mode (ν_6), is also possible.

Table 2

Vibrational progressions and assignments in the 7.0–7.6 eV absorption band of CF_3I (energies in eV)

Previous work		This work	Assignments
[3]	[7]		
7.126	7.126	7.126	ν_{00}
7.155	7.155	7.155	ν_3
7.184	7.184	7.182	$2\nu_3$
(?)	–	7.191	$2\nu_6$ (?)
7.211	7.210	7.211	ν_2
–	–	7.216	$3\nu_3$
–	–	7.243	$4\nu_3$
7.246	7.246	7.247	ν_1
–	–	7.262	$4\nu_6$ (?)
7.275	7.275	7.275	$5\nu_3$ (?) $\{\nu_1 + \nu_3\}$
7.292	7.293	7.292	$2\nu_2$
7.304	–	7.298	$6\nu_3$ (?) $\{\nu_1 + 2\nu_3\}$
–	–	7.311	??
7.330	7.329	7.331	$\nu_1 + \nu_2$
–	–	7.335	$7\nu_3$ (?)
–	–	7.357	??
–	–	7.363	$8\nu_3$ (?)
7.366	–	7.366	$2\nu_1$
7.372	–	7.372	$3\nu_2$
–	–	7.388	$4\nu_5$
7.394	–	7.394	$9\nu_3$ (?) $\{2\nu_1 + \nu_3\}$
–	–	7.401	$3\nu_2 + \nu_3$
7.408	–	7.412	$\nu_1 + 2\nu_2$
7.423	–	7.427	$10\nu_3$ (?) $\{2\nu_1 + 2\nu_3\}$
–	–	7.438	$3\nu_2 + 2\nu_3$
7.447	–	7.445	$2\nu_1 + \nu_2$
–	–	7.452	$11\nu_3$ (?) $\{2\nu_1 + 3\nu_3\}$
–	–	7.477	$12\nu_3$ (?)
7.484	–	7.488	$3\nu_1$
7.513	–	7.517	$3\nu_1 + \nu_3$
7.562	–	7.563	$3\nu_1 + \nu_2$

Assignments within brackets $\{\cdot\}$ are reported by [3,7]. (?) Indicates some uncertainty as to the classification; see discussion in the text. (??) Indicates there is no suggested assignment.

Peaks between 7.126 and 7.478 eV are regularly spaced by about ~ 0.03 eV (Fig. 1(a) and Table 3). We suggest that this series (comprising at least 12 members—Table 3) constitutes a vibrational progression in the C–I stretching mode, ν_3 , with a frequency of 0.029 eV; this value being close to the vibrational energy in the ground state (0.036 eV). Assignments for these peaks given by Sutcliffe and Walsh [3] are also listed in Table 2, in contrast they ascribe the features as arising from $\nu_1 + \nu_3$ overtones.

Table 3
Vibrational progressions in the 7.0–7.6 eV absorption band of CF₃I (energies in eV)

<i>n</i>	<i>n</i> ν ₃	Δ <i>E</i> (ν ₃)
0	7.126	–
1	7.155	0.029
2	7.182	0.027
3	7.216	0.034
4	7.243	0.027
5	7.275	0.032
6	7.298	0.023
7	7.335	0.037
8	7.363	0.028
9	7.394	0.031
10	7.427	0.033
11	7.452	0.024
12	7.478	0.026

Structures observed at energies below 7.126 eV peak are assigned to hot bands and confirm results of earlier authors [3,7,19]. The structure at 7.098 eV (approx. –0.028 eV) is a band involving excitation of ν₆, ground state frequency 0.033 eV [7]; the peak at 7.092 eV (approx. –0.034 eV) maybe attributed to ν₃ and that at 7.035 eV assigned as ν₂. The peak at 7.062 eV has been assigned as a ν₆ (0.064 eV) hot band and reported before as a probable 2ν_{6–0} transition [3]. A number of other hot bands can be identified at 7.086, 7.082, 7.070, 7.041, and 7.030 eV.

Other features at 7.133, 7.149, 7.161, 7.176, and 7.191 eV, as well as the observed shoulder to the left to the main peak, are attributed as sequence bands [3]. Fuss [5] suggesting that each ground state absorption has a hot band precursor, with ~0.007 eV (50 cm^{–1}) lower energy.

A low intensity peak at 7.191, 0.065 eV above the origin is also observed (Fig. 1(a)). The low vibrational energy leads us to ascribe it to the F₃–C–I bending mode, ν₆, 0.033 eV (262 cm^{–1}) in the ground state [7]. This mode being nonsymmetric, two quanta must be excited. Some broad structure at 7.209, 0.083 eV above the origin is tentatively assigned as an excited vibrational mode of ν₂, in the ²E_{3/2} [1] [7] state with a frequency of 681 cm^{–1} (0.085 eV).

The feature at 7.251, 0.125 eV above the 0–0 transition we assign as arising from C–F symmetric stretch

Table 4
Vibrational progressions and assignments in the 7.6–8.3 eV absorption band of CF₃I (energies in eV)

[3]	This work	Assignments
7.754	7.757	ν ₀₀
7.779	7.782	ν ₃
7.804	7.809	2ν ₃
7.827	7.831	ν ₂
7.852	7.853	ν ₂ + ν ₃
7.868	7.873	ν ₁
7.893	7.898	ν ₁ + ν ₃
–	7.946	ν ₁ + ν ₂ (?)
–	7.967	ν ₁ + ν ₂ + ν ₃ (?)
7.982	7.985 (7)	2ν ₁
–	8.010	2ν ₁ + ν ₃

Assignments within brackets (?) means uncertainty.

mode, ν₁, 0.121 eV (974 cm^{–1}) in the ²E_{3/2} [2] 6p excited state [8]; that at 7.269 eV (0.143 eV above the origin) was previously assigned [21] as a hot band resulting from the superposition of mode ν₁ and an excited state of ν₃; the peak at 7.281 eV (0.155 eV (~1250 cm^{–1})) above the 0–0 transition has been assigned previously [7] as arising from the excitation of ν₄.

3.4. The C band

The C band has its origin at 7.757 eV (Fig. 1(b)) and has been assigned to the ²E_{1/2} [1] state. Peaks assignments and their relative energies are tabulated and compared with other literature data [3] in Table 4. We observe increased broadening of the lines relative to the B band as first reported by Sutcliffe and Walsh [3]. An explanation for this could be due to predissociation such that discrete vibrational structure is replaced by a broad continuum. Such an explanation is supported by presence of the smooth, low-resolution feature around 7.830 eV, which may mark the crossing to the dissociative curve. The structures at energies below the 7.757 eV peak are once again assigned to hot bands.

Weak features are observed at 8.531 and 8.641 eV, before a strong peak at 8.760 eV signifies excitation of a new transition. Peaks assignments have been tentatively made (Table 5) and suggest a vibrational progression of ν₃. Once again the structure in this band

Table 5
Vibrational progressions and assignments in the 8.5–9.1 eV absorption band of CF₃I (energies in eV)

[3]	This work	Assignments
8.757	8.760	ν_{00}
8.785	8.788	ν_3
8.813	8.816	$2\nu_3$
–	8.841	$3\nu_3$
8.846	8.851	ν_2
–	8.876	$4\nu_3$
8.875	8.879	ν_1
–	8.905	$5\nu_3$
–	8.934	$6\nu_3$
8.936	8.940	$2\nu_2$
–	8.963	$7\nu_3$
8.964	8.969	$\nu_1 + \nu_2$
–	8.992	$8\nu_3$
8.993	8.996	$2\nu_1$
9.021	9.021	$9\nu_3$ (?) $\{2\nu_1 + \nu_3\}$
9.057	9.061	$\nu_1 + 2\nu_2$

The assignment within brackets {·} is reported by [3]. (?) Indicates some uncertainty as to the classification; see discussion in the text.

is similar to that observed for the 7.126 eV (B band) transition and we therefore, attribute the transition in the same way but with 6ss orbital being replaced by a more highly excited Rydberg orbital, 7ss.

Between 9.148 and 9.337 eV, there is evidence for the excitation of yet another electronic state but due to the broadness of the absorption lines it is not possible to define accurately the associated vibrational patterns. At 9.373 eV another band is observed that is analogous to the C-band transition with two ν_3 vibrational features at 9.397 and 9.429 eV. The 9.373 eV feature may correspond to the 8.760 eV transition but with $^2\Pi_{3/2}$ replaced by $^2\Pi_{1/2}$. The separation of 0.613 eV between these features is in agreement with that predicted by Sutcliffe and Walsh [3], suggesting energy splitting due to spin–orbit coupling. The 9.48 eV is the beginning of another band and above this energy several diffuse bands can occur every ~ 0.1 eV, underlying these peaks is broad band continuum absorption with a local maximum at 9.638 eV.

The first ionisation energy is at ~ 10.41 eV [3] such that both the 8.757 and 9.462 eV transitions must represent consecutive members of a Rydberg series leading to the lowest state of the CF₃I ion; partially

resolved structures are observed in the cross-section above 10.0 eV showing evidence of, at least, ν_1 and ν_3 vibrational series (Fig. 1(e)) for the neutral and ionic states, and is in agreement with previous work [23].⁴

3.5. Electron energy loss spectra (EELS)

The electron energy loss spectra shown in Fig. 2 agree well with the optical data, all the major photo-absorption bands are observed by EELS although the vibrational progression are not always observed due to the inherent lower resolution of EELS compared to photon techniques.

EELS is a very adaptable technique that has been used over a large number of years to measure the spectroscopy of atomic and molecular targets in both gas and solid phases. Since by varying the scattering angle and incident energy it is possible to detect both optically allowed and forbidden transitions. An electron with sufficiently high energy (>100 eV) scattered at small angles ($\sim 0^\circ$) will induce an electric field at the molecule very similar to that of a photon pulse. The electric field interacts with the transition dipole of the molecule with electric dipole transitions being predominantly excited. Hence, in this configuration, the EELS experiment will closely approximate a photo-absorption experiment. The EELS methodology also has certain advantages over photo-absorption experiments, namely that a wide energy range from visible to VUV wavelengths is easily accessible without the need to change optical lamps or filters. In the present work EELS allows higher lying electronic states to be probed (e.g., above 10.5 eV where the transmission of the optical windows is greatly diminished).

The EELS spectrum is not directly comparable with photo-absorption data. In order to relate the two quantities it is necessary to use the following equation to convert the EELS data to differential oscillator strengths (DOS):

$$\frac{df}{dE} \propto \frac{E\Delta\theta}{R} \frac{I(E)}{\ln[1 + (\Delta\theta/\gamma^2)]}$$

⁴ This paper has been incorrectly referenced in previous works.

where $\gamma^2 = E^2/4T(T - E)$, df/dE is the DOS, T the incident electron energy, E the energy loss, $\Delta\theta$ is the acceptance angle, R the Rydberg constant and $I(E)$ is the intensity of the scattered electron beam. The DOS values are directly proportional to the photo-absorption cross-sections but are relative values as they are only proportional to the scattered electron flux of the beam. Normalising the derived DOS (cross-section) at one wavelength then allows the EELS data to be compared directly with the photo-absorption measurements. The EELS and DOS spectra obtained for CF_3I are shown in Fig. 4. Excellent agreement is found between the present ‘zero’ angle data collected at University College London and the measured photo-absorption data.

At lower incident energies forbidden transitions will be more visible in the EEL Spectra. Fig. 2(b) shows energy loss spectra recorded at 100 eV incident energy and at a scattering angle of 3° compared a spectrum recorded at 30 eV and 15° . Above 7 eV, the spectra are in good agreement confirming that the transitions for bands B and C are allowed. However, notable differ-

ences are observed in band A (Fig. 2(b)) suggesting that the contributing electron states have some forbidden character.

At higher energies the EELS data suggest a series of absorption bands above 10.5 eV for which there is currently no information, a full electronic structure calculation deriving the energies of high lying Rydberg series would therefore be welcome. High resolution photon experiments at these short wavelengths may reveal vibrational structure which will assist in the classification of such features.

4. Conclusions

A detailed experimental investigation of the electronic states of CF_3I has been performed and confirms the presence of three absorption bands centred at 4.6, 7.12, and 7.75 eV with three further bands being found at 8.8, 9.6, and 10.3 eV. The electronic transitions can be assigned to be the components of a $5p\pi-6s$ Rydberg excitation. High resolution VUV

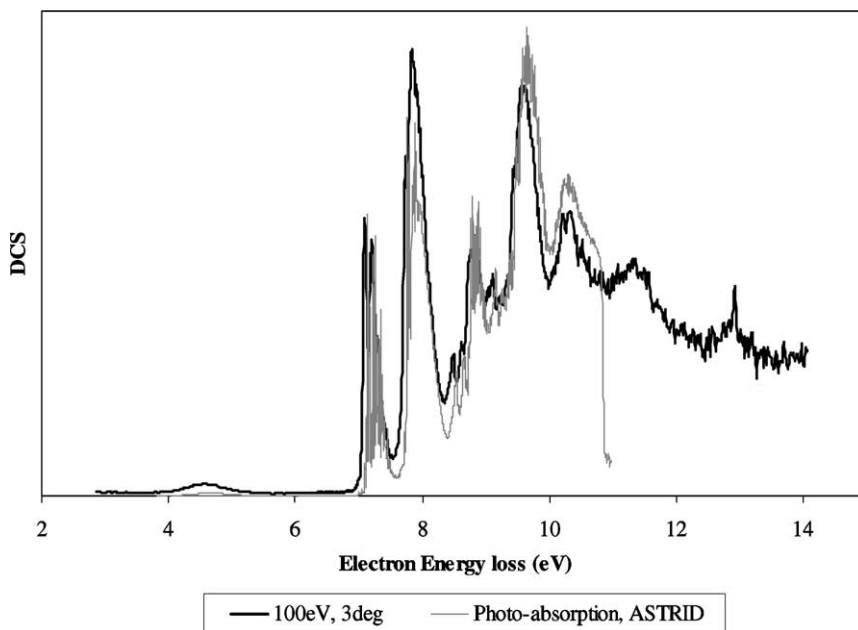


Fig. 4. Photo-absorption cross-sections derived from EELS measurements compared to those collected using the ASTRID synchrotron facility.

photo-absorption spectra reveal rich vibrational progressions involving excitation of the symmetric C–F, C–F₃ and C–I modes.

The first excitation observed (the A band with a maximum at 4.6 eV) arises from an $n \rightarrow \sigma^*$ transition and due to the spin–orbit coupling and exchange interactions is split into four components, ${}^2E_{3/2}$ and ${}^2E_{1/2}$ with projections of the total electronic angular momentum Ω of 2, 1, 0, 1. The resultant excited states are therefore dissociative along the C–I stretch coordinate.

The next excitation (onset 7.126 eV) can arise from a $n \rightarrow 6s$ transition, giving rise to four Rydberg excited states: ${}^2E_{3/2}$ [2], ${}^2E_{3/2}$ [1], ${}^2E_{1/2}$ [0] and ${}^2E_{1/2}$ [1], each one being further split by a relatively small exchange splitting, previously identified as \tilde{C} and \tilde{D} states [7].

The next excitation band arises from a $\sigma \rightarrow \sigma^*$ valence transition in the C–I bonding region, and due to a large exchange splitting resulting 3A_1 and 1A_1 states, the former being split into 3A_1 [1] and 3A_1 [0] components [7] (Table 1). The 3A_1 state has been identified with the \tilde{B} state observed by Robin [20] (6.356 eV), and calculated by Taatjes et al. to be at 6.154 eV. The dissociative state $\sigma \rightarrow \sigma^* {}^1A_1$ is close to the ${}^2E_{1/2}$ ion core states of the $n \rightarrow 6s$ transition and predissociation may occur along the C–I stretch coordinate as discussed by Robin [24].

The photo-absorption cross-section has been measured using two different methodologies, and for the first time below 200 nm. However, present photo-absorption cross-section values for the A band are in disagreement with one another by some 10%, hence the present measurements cannot distinguish between the discrepancies in previous work. In view of this and its importance in plasma reactor design it is suggested that other workers should measure these cross-sections. A full calculation on the electronic state structure of CF₃I is also needed.

Acknowledgements

N.J.M., A.D., S.E., P.K. acknowledge the support of UK funding councils EPSRC, NERC and CLRC

during the course of this research. P.T. also thanks the EU for provision of a Marie Curie Fellowship and P.L.V. the Portuguese “Fundação para a Ciência e a Tecnologia” for a Postgraduate Scholarship. H.T. also gratefully acknowledges the warm hospitality extended to him by Professor S.J. Buckman during a sabbatical at the Australian National University, Canberra where part of this paper was prepared. S.M.S. would like to acknowledge a financial grant from Royal Society of London/National Hellenic Research Foundation that made his visit to UCL possible.

References

- [1] H. Tanaka, M. Inokiti, *Adv. Atom. Mol. Opt. Phys.* 43 (2000) 1.
- [2] S. Samukawa, Mukai, *J. Vac. Sci. Technol.* A17 (1999) 5.
- [3] L.H. Sutcliffe, A.D. Walsh, *Trans. Faraday Soc.* 57 (1961) 873.
- [4] G. Herzberg, *Discuss. Faraday Soc.* 35 (1963) 7.
- [5] W. Fuss, *J. Chem. Phys.* 86 (1982) 731.
- [6] I. Powis, O. Dutuit, M. Richard-Viard, P.M. Guyon, *J. Chem. Phys.* 92 (1990) 1643.
- [7] C.A. Taatjes, J.W.G. Mastenbroek, G. van den Hoek, J.G. Snijders, S. Stolte, *J. Chem. Phys.* 98 (1993) 4355.
- [8] N.A. Macleod, S. Wang, J. Hennessy, T. Ridley, K.L. Lawley, R.J. Donovan, *J. Chem. Faraday Trans.* 94 (1998) 2689.
- [9] A. Fahr, A.K. Nayak, R. Huie, *Chem. Phys.* 199 (1995) 275.
- [10] O.V. Rattigan, D.E. Shallcross, R.A. Cox, *J. Chem. Soc., Faraday Trans.* 93 (1997) 2839.
- [11] S. Solomon, J.B. Burkholder, A.R. Ravishankara, R.R. Garcia, *J. Geophys. Res.* 99 (1994) 20929.
- [12] N.J. Mason, J.M. Gingell, J.A. Davis, H. Zhao, I.C. Walker, M.R.F. Siggel, *J. Phys. B* 29 (1996) 3075.
- [13] J.M. Gingell, N.J. Mason, H. Zhao, I.C. Walker, M.R.F. Siggel, *J. Phys. B* 32 (1999) 5229.
- [14] J.A. Davies, N.J. Mason, G. Marston, R.P. Wayne, *J. Phys. B* 28 (1995) 4179.
- [15] N.J. Mason, J.M. Gingell, J.A. Davis, *Physica Magazine* 17 (1995) 113.
- [16] W.M. Johnstone, N.J. Mason, W.R. Newell, P. Biggs, G. Marston, R.P. Wayne, *J. Phys. B* 25 (1992) 3873.
- [17] H. Tanaka, T. Ishikawa, T. Masai, T. Sagara, L. Boesten, M. Takekawa, Y. Itikawa, M. Kimura, *Phys. Rev. A* 57 (1998) 1798.
- [18] G. Herzberg, *Molecular Spectra and Molecular Structure*, vol. III: *Electronic Spectra of Polyatomic Molecules*, ed. Van Nostrand Reinhold, New York, 1966.
- [19] R.S. Mulliken, E. Teller, *Phys. Rev.* 61 (1942) 283; D.H. Parker, R. Pandolfi, P.R. Stannard, M.A. El-Sayed, *Chem. Phys.* 45 (1979) 27.

- [20] M.B. Robin, Higher Excited States of Polyatomic Molecules, vol. I, Academic Press, New York, 1974;
M.B. Robin, *Can. J. Chem.* 63 (1985) 2032.
- [21] G. van den Hoek, J.W. Thoman Jr., D.W. Chandler, S. Stolte, *Chem. Phys. Lett.* 188 (1992) 413.
- [22] L.D. Waits, R.J. Horwitz, R.G. Daniel, J.A. Guest, J.R. Appling, *J. Chem. Phys.* 97 (1992) 7263.
- [23] T. Cvitaš, H. Güsten, L. Klasinc, I. Novadj, H. Vanèik, *Z. Naturforsch.* 32a (1977) 1528.
- [24] M.B. Robin, *Can. J. Chem.* 63 (1985) 2032.